Fast Nuclear Spin Relaxation in Hyperpolarized Solid ^{129}Xe

N. N. Kuzma, B. Patton, K. Raman, and W. Happer

Joseph Henry Laboratory, Department of Physics, Princeton University, Princeton, New Jersey 08544

(Received 15 January 2002; published 22 March 2002)

We report extensive new measurements of the longitudinal relaxation time T_1 of ^{129}Xe nuclear spins in solid xenon. For temperatures $T < 120$ K and magnetic fields $B > 0.05$ T, we found T_1 on the order of hours, in good agreement with previous measurements and with the predicted phonon-scattering limit for the spin-rotation interaction. For $T > 120$ K, our new data show that T_1 can be much shorter than the phonon scattering limit. For $B = 0.06$ T, a field often used to accumulate hyperpolarized xenon, T_1 is ~6 s near the Xe melting point $T_m = 161.4$ K. From $T = 50$ K to T_m, the new data are in excellent agreement with the theoretical prediction that the relaxation is due to (i) modulation of the spin-rotation interaction by phonons, and (ii) modulation of the dipole-dipole interaction by vacancy diffusion.

DOI: 10.1103/PhysRevLett.88.147602 PACS numbers: 76.60.Es, 75.40.Gb

In recent years, optical pumping [1] has been successfully used to prepare large quantities of hyperpolarized noble gases ^{3}He [2] and ^{129}Xe [3]. The applications range from inelastic electron scattering [4] and searches for nuclear electric-dipole moments [5] to enhancement of nuclear magnetic resonance (NMR) signals of surfaces [6], solutions [7], and air spaces such as human lungs. High-resolution ^{3}He lung images have been reported [8], but the quality of ^{129}Xe imaging [9] is still limited by the comparatively low nuclear spin polarization (10%–15%) in xenon gas. On the other hand, highly polarized xenon is especially promising for medicine, where it can be used as a potential chemical-shift probe of human tissues [10].

A number of recent studies [11] have focused on the gas-phase physics of producing hyperpolarized ^{129}Xe by spin-exchange optical pumping. Much less is known about what happens to ^{129}Xe spins during the subsequent cryogenic separation of Xe from much larger quantities of He and N_2 buffer gases currently used [3] for efficient optical pumping. Despite experimental evidence [12,13] that a small amount of hyperpolarized xenon preserves almost all of its polarization after a freeze/thaw cycle in a sealed cell, currently about half of ^{129}Xe polarization is lost during cryogenic separation and accumulation.

To improve the performance of hyperpolarized xenon accumulators, a better fundamental understanding of the causes of longitudinal ^{129}Xe spin relaxation is needed. There have been NMR studies of ^{129}Xe in Xe gas [14], Xe liquid [15], and Xe-N_2 liquid solution [16]. ^{129}Xe spin relaxation in pure gaseous and liquid xenon is known to be caused by the spin-rotation interaction [17],

$$V_{\rm sr} = c_K(r_{\alpha\beta})\mathbf{I}_\alpha \cdot \mathbf{N}_{\alpha\beta}\,, \tag{1}$$

between the nuclear spin $\mathbf{I}_\alpha$ of a ^{129}Xe atom α and the relative angular momentum $\mathbf{N}_{\alpha\beta}$ of the atom pair that also involves a second xenon atom β, with or without spin, located a distance $r_{\alpha\beta}$ away. The interaction (1) was also found to be responsible for spin relaxation of ^{129}Xe at temperatures $50 \lesssim T \lesssim 120$ K, where it gives rise to the Raman scattering of phonons in solid xenon [18]. The spin-rotation coupling coefficient c_K decreases so rapidly (exponentially) with $r_{\alpha\beta}$ that one need only consider the nearest-neighbor interactions in the crystal.

The familiar nuclear dipole-dipole interaction [19],

$$V_{\rm dd} = \frac{\mu_\alpha \mu_\beta}{I_\alpha I_\beta r_{\alpha\beta}^3}\left[\mathbf{I}_\alpha \cdot \mathbf{I}_\beta - 3\,\frac{(\mathbf{I}_\alpha \cdot \mathbf{r}_{\alpha\beta})(\mathbf{r}_{\alpha\beta} \cdot \mathbf{I}_\beta)}{r_{\alpha\beta}^2}\right], \tag{2}$$

may mediate cross-relaxation between ^{129}Xe and ^{131}Xe [18,20] below 50 K. With this exception, however, the relaxation of ^{129}Xe in gaseous and liquid xenon, as well as over a wide temperature range in solid xenon, was thought to be mediated by the spin-rotation interaction of Eq. (1).

Here we present extensive NMR measurements of the longitudinal spin relaxation time T_1 in hyperpolarized solid ^{129}Xe. We show that, for temperatures above 120 K, T_1 can be several orders of magnitude shorter than what is expected from phonon scattering mediated by the spin-rotation interaction of Eq. (1). The observed additional relaxation is in excellent quantitative agreement with the predicted effects of the dipole-dipole interaction of Eq. (2), modulated by vacancy diffusion [21,22], both for samples of natural isotopic composition and for samples highly enriched in ^{129}Xe.

In this experiment, xenon gas was polarized with a prototype commercial system (model IGI.9800.Xe polarizer, Magnetic Imaging Technologies) connected via a pair of nylon tubes to a glass cold finger (Fig. 1, *A*) in a setup described elsewhere [16]. The cold finger was placed in a cryostat, cooled by a stream of He gas coming from the liquid helium bath of a superconducting magnet system (Oxford Instruments). The standard He-N_2-Xe gas mixture (~1% Xe of either natural isotopic composition, 26.4% ^{129}Xe and 21.2% ^{131}Xe, or isotopically enriched, 86% ^{129}Xe and 0.13% ^{131}Xe) was polarized and flowed at a pressure of 4.5 atm through the cold finger, maintained at $T \sim 60$ K, for a 30–50 min accumulation period. The pressure was then lowered to ~1.5 atm, and the cryostat was warmed to 190 K and immediately cooled back down to a desired temperature. The goal was to liquefy the ac-

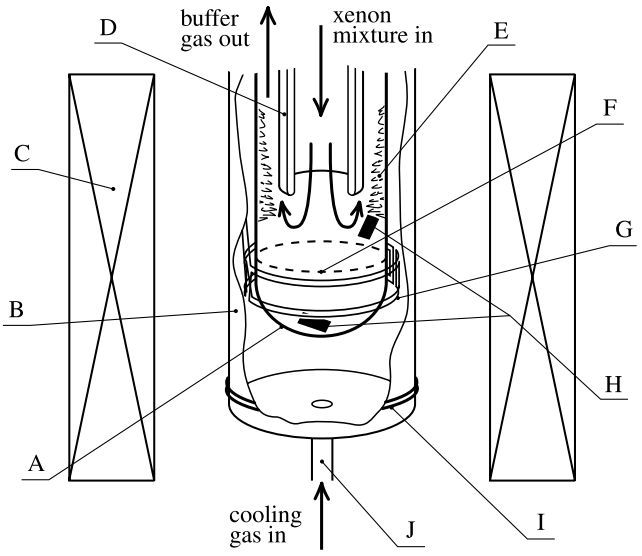

FIG. 1. Schematic diagram of the experimental setup (not to scale). The pressurized gas mixture with hyperpolarized ^{129}Xe flows through the glass accumulator (A), placed into the cryostat insert (B) inside a superconducting magnet (C). The mixture comes in through the inlet tube (D), kept just above the Xe melting temperature T_m. As the mixture flow turns around and comes in contact with the cold glass walls of the accumulator, xenon is deposited in the form of snow (E). Once the accumulation is completed, xenon snow is heated above T_m, melts, and fills the bottom of the accumulator to the level shown by the dashed line (F). After xenon is recrystallized, NMR signals are detected by a two-turn surface coil (G). The temperature, monitored by sensors (H), can be controlled using a counterwound heater (I) and a valved cooling gas inlet (J).

cumulated Xe snow (Fig. 1, E), so it could run down and refreeze as a dense solid. At the same time we tried to warm xenon past its melting point quickly, especially at low fields, to avoid rapid relaxational loss of polarization.

To obtain data at the lowest fields, accumulation and refreezing of xenon were performed at $B = 1.435$ T. The magnet was then brought down to the desired field and the superconducting shim coils (that provide the field homogeneity) were set quickly to the predetermined values. At $B = 0.067$ T, an internal NMR coil of poorer stability had to be used, resulting in larger T_1 errors. The temperature T was controlled with a heater (Fig. 1, I), using two Cernox^{TM} thin-film resistor sensors (model CX-1080-BG-HT, Lake Shore), calibrated to ± 0.1 K and suspended inside the cold finger 2 cm one above the other. Over weeks of use, the bottom sensor calibration drifted by a small amount ($\lesssim 2$ K), determined from the $T(t)$ "plateau" at 161.4 K during melting/crystallization of xenon. Appropriate temperature corrections were made.

A two-turn NMR surface coil (Fig. 1, G) was mounted to enclose the region of the cold finger where magnetic field was homogeneous to ~ 3 μT. The coil was connected to the spectrometer [16] which applied weak 0.8–12 μs pulses, tipping ^{129}Xe spins by small angles (0.3°–5°) at regular intervals (15 s–8 min). Much longer pulses (up to 50 μs) were also used to estimate the effect of tipping on ^{129}Xe relaxation. The integral intensity A of thus obtained spectra was plotted as a function of time t. The resulting curves of relaxation to thermal equilibrium were fitted to an exponential $A(t) = A_0 \exp(-t/T_1)$. Each T_1 value was later corrected by a small amount ($<10\%$) for depolarization caused by the pulses.

Figure 2(a) shows the summary of our ^{129}Xe relaxation data (open symbols), taken in natural xenon at five different fields, from 0.067 T (squares) to 1.435 T (diamonds). Below 120 K our data are in good agreement with the earlier data (crossed circles) by Gatzke *et al.* [12], obtained in natural xenon at 0.1–0.2 T, and with the calculated effects (thick solid curve R) of the Raman scattering of phonons by ^{129}Xe nuclei [18]. Our new data extend all the way to the melting point of xenon (vertical dashed line), but are limited to $T_1 > 60$ s by our current apparatus. The T_1 values are reproducible over many cryogenic cycles, which indicates the validity of the data.

The observed spin relaxation times are in excellent agreement with the theoretically predicted values [Fig. 2(a), solid curves A–E], calculated from (i) the phonon scattering through the spin-rotation interaction (1), as described by Fitzgerald *et al.* [18], and (ii) the dipole-dipole interaction (2) [23], modulated by vacancy diffusion as described by Sholl [24,25]. The spin polarization of ^{131}Xe is always negligibly small compared to that of hyperpolarized ^{129}Xe, because of rapid ^{131}Xe relaxation due to its nuclear quadrupole moment [26], so the predicted spin relaxation rate of ^{129}Xe is

$$\frac{1}{T_1} = \frac{9\pi c_K^2 T^{*2} \eta^S(\epsilon_0, T^*)}{4\hbar^2 \omega_D} + f_I \frac{\hbar^2 \gamma_I^4 \tau I(I+1)}{5b^6} [g(\omega_I \tau/2) + 4g(\omega_I \tau)] + f_S \frac{\hbar^2 \gamma_I^2 \gamma_S^2 \tau S(S+1)}{15b^6} \{6g([\omega_I + \omega_S]\tau/2) + g([\omega_I - \omega_S]\tau/2) + 3g(\omega_I \tau/2)\}. \quad (3)$$

All parameters in Eq. (3) are well known from independent sources, and we have made no attempt to adjust them to make them fit our experimental data. The spin-rotation coupling coefficient is $c_K = h\nu$, with $\nu = -27$ Hz at 77 K; the parameter $\epsilon_0 = r_{\alpha\beta} d \ln|c_K|/dr_{\alpha\beta} = -11.8$ describes the nearly exponential dependence of c_K on the Xe pair separation [18]. The ratio of the temperature T to the Debye temperature $T_D = 55$ K of xenon is $T^* = T/T_D$, and $\omega_D = k_B T_D/\hbar$. The phonon-freeze-out factor, $\eta^S(\epsilon_0, T^*)$, is very nearly equal to its high-temperature limit $\eta^S(\epsilon_0, \infty) = 2686.8$ for $T > 50$ K [18]. The nuclear spin quantum numbers of ^{129}Xe and ^{131}Xe are $I = 1/2$ and $S = 3/2$, respectively. The gyromagnetic ratios (in units of 10^3 s^{-1} G^{-1}) are $\gamma_I = -\mu_I/I\hbar = 7.402$ and $\gamma_S = -\mu_S/S\hbar = -2.193$. The (radian) Larmor

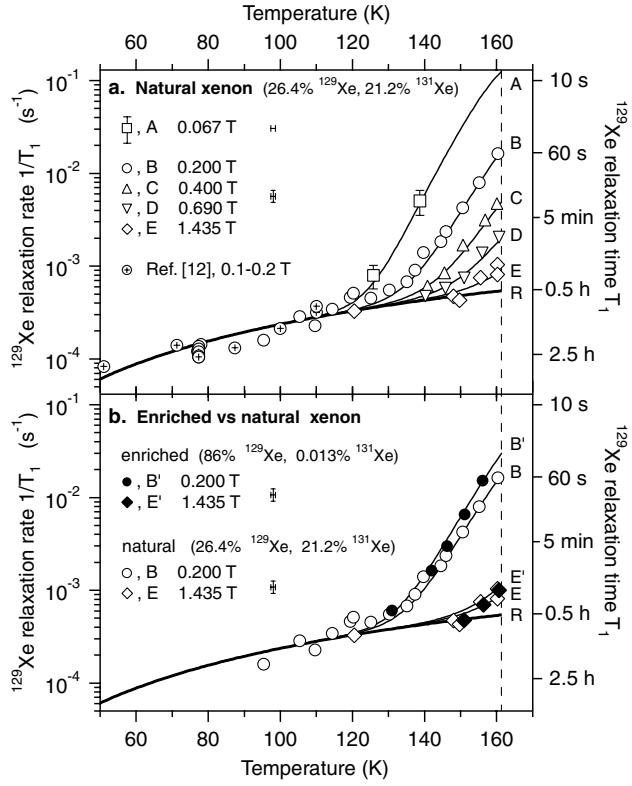

FIG. 2. ^{129}Xe nuclear spin relaxation measurements in natural and enriched xenon. Our new data [open symbols (natural Xe) and filled symbols (enriched Xe)] are in excellent quantitative agreement both with the earlier data at lower temperatures (crossed circles) and with the theoretical predictions of the combined effects of interactions (1) and (2) (solid curves A–E for natural xenon, and B', E' for enriched xenon) from ~50 K to the melting point $T_m = 161.4$ K (dashed line). The high-field relaxation limit corresponds to the Raman scattering of phonons (thick solid curve R). The absolute temperature errors and the relative $1/T_1$ errors are shown in the legend.

frequencies in an applied magnetic field B are $\omega_I = \gamma_I B$ and $\omega_S = \gamma_S B$. For xenon of natural isotopic composition the fractional abundances are $f_I = 0.264$ and $f_S = 0.212$. For 78 K $< T \leq T_m$, the lattice parameter of xenon crystals has been accurately measured with x-ray scattering by Granfors *et al.* [22]. Their data are well represented by the empirical formula (with b in Å and T in K) $b(T) = 6.276\,416 + 0.001\,807\,71(T - 125) + 4.576\,33 \times 10^{-6}(T - 125)^2$. The spin-rotation coupling was scaled as $c_K(T) = c_K(77\text{ K})\{1 + 300\text{ Å}^3[b^{-3}(T) - b^{-3}(77\text{ K})]\}$ to account for the density dependence [27] of the ^{129}Xe paramagnetic chemical shift, to which c_K is proportional. The hopping rate $1/\tau$ per Xe atom has been inferred by Yen and Norberg [21] from their temperature-dependent T_2 measurements of ^{129}Xe. Their findings can be interpolated as $\tau = 8.8 \times 10^{-17}$ s $\times \exp(3604\text{ K}/T)$. An analytic approximation for the dimensionless spectral density function, $g(y)$, in the monovacancy limit [25] is $g(y) = 55.5/(0.169 + 0.128\sqrt{y} + y^2)$.

Figure 2(b) compares our enriched Xe data (filled symbols) to the natural Xe data of Fig. 2(a), obtained at the same field values (0.200 and 1.435 T). The relaxation in samples enriched to 86% ^{129}Xe (only 0.13% ^{131}Xe) is also in excellent agreement with Eq. (3) (solid curves B', E'), and at 0.2 T is about 70% faster compared to samples of natural isotopic composition. Thus ^{131}Xe atoms are somewhat more effective than ^{129}Xe atoms at causing spin relaxation of ^{129}Xe nuclei. The magnetic moment of ^{131}Xe is smaller in magnitude than that of ^{129}Xe (0.69 vs -0.77 nm), and would therefore be less effective in causing relaxation. But the coupling frequencies ω in the spectral density functions $g(\omega)$ are smaller for ^{131}Xe, resulting in larger values $g(\omega)$ in Eq. (3) and, ultimately, in a slightly stronger effect of ^{131}Xe on relaxation of ^{129}Xe.

Finally, we use the data of Fig. 2(a) to model cryogenic accumulation of natural xenon at several practical values of magnetic field. We assume a solid xenon layer to be growing steadily under a fixed linear temperature increase across its width. The layer is in thermal contact with the glass wall at $T = 77$ K on one side, and with the flow of the warmer gas mixture on the other. We further assume that the temperature at the other side is fixed. To be consistent with observations [28] at 0.06 T, we take this temperature to be 145 K. Figure 3 shows the total magnetization of the growing layer as a function of time t. If there were no spin relaxation, the total magnetization would grow linearly with time, as more xenon is deposited (dotted line, normalized to 1 at $t = 120$ min). The four curves show the magnetization growth of the layer under relaxation effects shown in Fig. 2(a). Obvious advantages of accumulation at high fields are seen, both in polarization and in the amount of xenon that can be accumulated before its magnetization declines.

In summary, the relaxation of ^{129}Xe at temperatures above 50 K is well described by Eq. (3) which combines

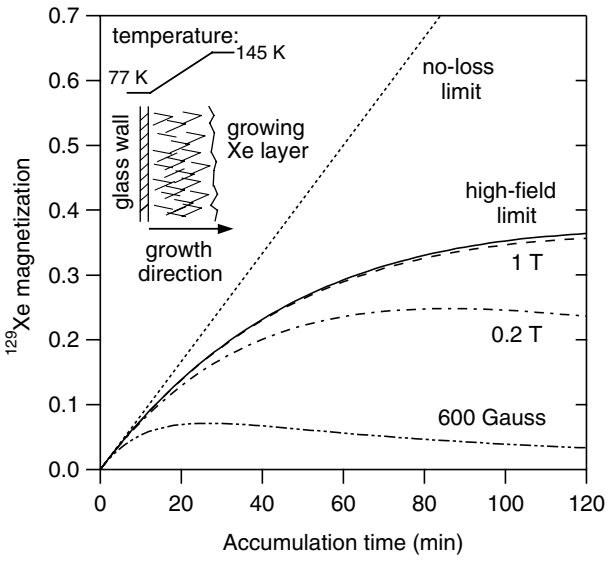

FIG. 3. A simple accumulator performance model, assuming linear temperature increase 77–145 K across the growing Xe layer. After 15 min of accumulation at 0.06 T (lowest curve), the magnetization is about 50% of the no-loss limit, consistent with 50% polarization losses observed by [28].

the effects of the spin-rotation interaction of Eq. (1) and the magnetic dipole-dipole interaction of Eq. (2). The details of the two mechanisms are different. The spin-rotation interaction (1) causes spin-flip Raman scattering of phonons, and the resulting relaxation rate is approximately proportional to the square of the temperature. Magnetic fields of a few tesla make little difference to the relaxation rate. Simple calculations show that (1) causes negligible relaxation when modulated by vacancy diffusion. This is because the interaction (1), unlike (2), is velocity dependent and its mean value is always zero, except for the short time needed for a vacancy to hop.

The magnetic dipole-dipole interaction of Eq. (2) causes ^{129}Xe relaxation when it is modulated by vacancy diffusion. It has a strong temperature dependence, because of the Arrhenius activation of the vacancy density and vacancy hopping rate. The relaxation can be strongly affected by ordinary laboratory fields of a tesla or less. On the other hand, estimates by Waller [29,30] show that relaxation caused by phonon scattering through the dipole-dipole interaction (2) is completely negligible.

We believe this is the first systematic study of spin relaxation due to vacancy diffusion in a hyperpolarized solid. The dependence of relaxation rates on temperature, magnetic field, and isotopic composition is reported for a system of two magnetic nuclear species. Semiquantitative evidence for ^{129}Xe relaxation due to vacancy diffusion was obtained by Cates *et al.* [31]. Some of these effects were also seen earlier in more complicated molecular solids CH_4 [32] and $(CH_2CN)_2$ [33]. The improved understanding of how the ^{129}Xe relaxation rate depends on temperature and magnetic field should help design better cryogenic accumulators of hyperpolarized ^{129}Xe.

We thank Bastiaan Driehuys for many helpful discussions and for arranging equipment loans. We are grateful to Colin Sholl for confirming that Eq. (3) is the appropriate generalization of translational diffusion theory to the case of unlike spins. We also thank Michael Souza for his expert glass-blowing. This work was supported by the U.S. Air Force Office of Scientific Research.

[1] T. G. Walker and W. Happer, Rev. Mod. Phys. **69**, 629 (1997).
[2] J. R. Johnson *et al.,* Nucl. Instrum. Methods Phys. Res., Sect. A **356**, 148 (1995); T. E. Chupp, M. E. Wagshul, K. P. Coulter, A. B. McDonald, and W. Happer, Phys. Rev. C **36**, 2244 (1987).
[3] B. Driehuys *et al.,* Appl. Phys. Lett. **69**, 1668 (1996).
[4] P. L. Anthony *et al.,* Phys. Rev. D **54**, 6620 (1996).
[5] M. V. Romalis and M. P. Ledbetter, Phys. Rev. Lett. **87**, 067601 (2001).
[6] T. Rõõm, S. Appelt, R. Seydoux, E. L. Hahn, and A. Pines, Phys. Rev. B **55**, 11 604 (1997).
[7] G. Navon *et al.,* Science **271**, 1848 (1996).
[8] H.-U. Kauczor *et al.,* J. Magn. Reson. Imaging **7**, 538 (1997); E. E. de Lange *et al.,* Radiology **210**, 851 (1999).
[9] J. P. Mugler *et al.,* Magn. Reson. Med. **37**, 809 (1997).
[10] K. Mazitov, A. N. Panov, K. M. Enikeev, and A. V. Il'yasov, Dokl. Biophys. **364–366**, 28 (1999).
[11] D. K. Walter, W. M. Griffith, and W. Happer, Phys. Rev. Lett. **88**, 093004 (2002); *ibid.* **86**, 3264 (2001); C. J. Erickson *et al., ibid.* **85**, 4237 (2000).
[12] M. Gatzke *et al.,* Phys. Rev. Lett. **70**, 690 (1993).
[13] U. Ruth, T. Hof, J. Schmidt, D. Fick, and H. J. Jansch, Appl. Phys. B **68**, 93 (1999).
[14] R. L. Streever and H. Y. Carr, Phys. Rev. **121**, 20 (1961); H. C. Torrey *ibid.* **130**, 2306 (1963); D. Brinkmann, E. Brun, and H. H. Staub, Helv. Phys. Acta **35**, 431 (1962); C. J. Jameson, A. K. Jameson, and S. M. Cohen, J. Chem. Phys. **59**, 4540 (1973); I. L. Moudrakovski *et al., ibid.* **114**, 2173 (2001).
[15] K. L. Sauer, R. J. Fitzgerald, and W. Happer, Chem. Phys. Lett. **277**, 153 (1997).
[16] B. Patton, N. N. Kuzma, and W. Happer, Phys. Rev. B **65**, 020404 (2002).
[17] N. F. Ramsey, Phys. Rev. **78**, 699 (1950).
[18] R. J. Fitzgerald, M. Gatzke, D. C. Fox, G. D. Cates, and W. Happer, Phys. Rev. B **59**, 8795 (1999).
[19] N. Bloembergen, E. M. Purcell, and R. V. Pound, Phys. Rev. **73**, 679 (1948); C. P. Slichter, *Principles of Magnetic Resonance* (Springer-Verlag, Berlin, 1990).
[20] S. Lang, I. L. Moudrakovski, C. I. Ratcliffe, J. A. Ripmeester, and G. Santyr, Appl. Phys. Lett. **80**, 886 (2002).
[21] W. Y. Yen and R. E. Norberg, Phys. Rev. **131**, 269 (1963).
[22] P. R. Granfors, A. T. Macrander, and R. O. Simmons, Phys. Rev. B **24**, 4753 (1981).
[23] A. Abragam, *Principles of Nuclear Magnetism* (Oxford University Press, Oxford, 1961).
[24] C. A. Sholl, J. Phys. C **7**, 3378 (1974).
[25] C. A. Sholl, J. Phys. C **21**, 319 (1988).
[26] W. W. Warren and R. E. Norberg, Phys. Rev. **148**, 402 (1966); R. E. Norberg, Springer Tracts Mod. Phys. **103**, 59 (1984).
[27] D. Brinkmann and H. Y. Carr, Phys. Rev. **150**, 174 (1966); D. F. Cowgill and R. E. Norberg, Phys. Rev. B **6**, 1636 (1972).
[28] B. Driehuys (private communication).
[29] I. Waller, Z. Phys. **79**, 370 (1932).
[30] N. Bloembergen, Physica **15**, 386 (1949).
[31] G. D. Cates *et al.,* Phys. Rev. Lett. **65**, 2591 (1990).
[32] G. A. De Wit and M. Bloom, Can. J. Phys. **43**, 986 (1965).
[33] J. G. Powles, A. Begum, and M. O. Norris, Mol. Phys. **17**, 489 (1969).